Asian Journal of Atmospheric Environment
Vol. 11, No. 4, pp. 300-312, December 2017
doi: https://doi.org/10.5572/ajae.2017.11.4.300
ISSN (Online) 2287-1160, ISSN (Print) 1976-6912

Observation of Secondary Organic Aerosol and New Particle Formation at a Remote Site in Baengnyeong Island, Korea

Jinsoo Choi, Yongjoo Choi[1)], Junyoung Ahn, Jinsoo Park, Jun Oh, Gangwoong Lee[1)], Taehyun Park[1)], Gyutae Park[1)], Jeffrey S. Owen[1)] and Taehyoung Lee[1),*]

Climate & Air Quality Research Department, National Institute of Environmental Research, Incheon, Republic of Korea
[1)]Department of Environmental Science, Hankuk University of Foreign Studies, Yongin, Republic of Korea

*Corresponding author. Tel: +82-31-330-4039, E-mail: thlee@hufs.ac.kr

ABSTRACT

To improve the understanding of secondary organic aerosol (SOA) formation from the photo-oxidation of anthropogenic and biogenic precursors at the regional background station on Baengnyeong Island, Korea, gas phase and aerosol chemistries were investigated using the Proton Transfer Reaction Time of Flight Mass Spectrometer (PTR-ToF-MS) and the Aerodyne High Resolution Time of Flight Aerosol Mass Spectrometer (HR-ToF-AMS), respectively. HR-ToF-AMS measured fine particles (PM_1; diameter of particle matter less than 1 μm) at a 6-minute time resolution from February to November 2012, while PTR-ToF-MS was deployed during an intensive period from September 21 to 29, 2012. The one-minute time-resolution and high mass resolution (up to 4000 m Δm^{-1}) data from the PTR-ToF-MS provided the basis for calculations of the concentrations of anthropogenic and biogenic volatile organic compounds (BVOCs) including oxygenated VOCs (OVOCs). The dominant BVOCs from the site are isoprene (0.23 ppb), dimethyl sulphide (DMS, 0.20 ppb), and monoterpenes (0.38 ppb). Toluene (0.45 ppb) and benzene (0.32 ppb) accounted for the majority of anthropogenic VOCs (AVOCs). OVOCs including acetone (3.98 ppb), acetaldehyde (2.67 ppb), acetic acid (1.68 ppb), and formic acid (2.24 ppb) were measured. The OVOCs comprise approximately 75% of total measured VOCs, suggesting the occurrence of strong oxidation processes and/or long-range transported at the site. A strong photochemical aging and oxidation of the atmospheric pollutants were also observed in aerosol measured by HR-ToF-AMS, whereby a high $f_{44} : f_{43}$ value is shown for organic aerosols (OAs); however, relatively low $f_{44} : f_{43}$ values were observed when high concentrations of BVOCs and AVOCs were available, providing evidence of the formation of SOA from VOC precursors at the site. Overall, the results of this study revealed several different SOA formation mechanisms, and new particle formation and particle growth events were identified using the powerful tools scanning mobility particle sizer (SMPS), PTR-ToF-MS, and HR-ToF-AMS.

Key words: HR-ToF-AMS, PTR-ToF-MS, Baengnyeong Island, Volatile organic compounds, Photochemical reaction

1. INTRODUCTION

Particulate matter can be comprised of a large amount of organic materials at not only urban/regional area, but also remote sites (Jimenez *et al*., 2009; Zhang *et al*., 2006; Andrews *et al*., 2000; Chow *et al*., 1994). During the past decades, there are significant development of the characterization of organic aerosols (OAs) along with their emission sources and effect on the environment. Previous studies have improved the understanding for the contribution of organics to fine particulate matter, and the negative corresponding health effects have consequently been elucidated (Ostro and Chestnut, 1998). OAs play an important role in the Earth's radiation balance by scattering or absorbing sunlight in direct and by acting role of cloud condensation nuclei in indirectly (Charlson *et al*., 1992). Further, the existence of organic materials in atmospheric aerosol enhanced the ability of the internally mixed aerosol particles to serve as CCN due to its hygroscopicity (Kumar *et al*., 2003; Prenni *et al*., 2003, 2001; Giebl *et al*., 2002; Raymond and Pandis, 2002; Corrigan and Novakov, 1999).

Because OAs influence on both air quality and climate, it is worthwhile to distinguish the anthropogenic

contribution from the natural background in order to address the future regulatory guidance that may be implemented to lower the emissions contributing to the OAs burden. Usually, regulation targets the control of various kinds of emissions such as secondary organic aerosol (SOA) precursors, nitrogen oxides (NO_x), mass concentrations of sulfate or particulate matter. Before the implementation of emission controls, chemical transport models (CTMs) are used at a regional and/or global scales to evaluate the effects of changes in emissions on the OAs burden. In large scale CTMs, OAs have commonly been classified into two groups, as follows: essentially non-volatile species emitted as primary organic aerosol (POA), and volatile compounds that oxidize and then partition to the condensed phase in the atmosphere as SOA (Hoyle *et al*., 2007; Tsigaridis and Kanakidou, 2003; Chung and Seinfeld, 2002). According to recent studies, POA is more volatile than SOA (Huffman *et al*., 2009; Robinson *et al*., 2007), but the designation of POA as unreacted and generally reduced primary emissions is still valid (Donahue *et al*., 2009). A source-based classification of anthropogenic POA (APOA) and anthropogenic SOA (ASOA) were investigated, and proposed a set of measurable distinguishing characteristics for the carbonaceous aerosols in these groups (Fuzzi *et al*., 2006). Typically, anthropogenic OAs emitted from fossil fuel combustion, meat cooking, biomass burning, and other human activities that lead to the emission of both fossil and modern (i.e. not fossil) volatile organic carbon. As a result, modern OAs should be distinguished between anthropogenic and biogenic fractions. However, even if it is determined that a fraction of modern volatile organic compounds (VOCs) is actually being emitted from anthropogenic sources, it does not capture the whole human influence on the OAs budget, as it ignores any possible enhancement, through anthropogenically emitted compounds, of the SOA formation from true biogenic precursors.

Despite the level of understanding for the formation process of SOA are still low, SOA forms from oxidized VOC precursor gases, mainly by OH radicals for anthropogenic VOC (AVOC) during the daytime, and NO_3 and O_3 for biogenic VOC (BVOC) during nighttime (Matsui *et al*., 2009). The oxidation process adds functional groups to the organic gas molecules, resulting in decrease of their vapor pressure. This process partly results in gases that are again volatile and do not contribute to the aerosol formation; however, if the ambient conditions are favourable, another semi-volatile part of the reaction products might condense to form aerosols.

The current SOA models, however, are hard to simulate characteristics of measured OAs concentrations (Heald *et al*., 2005; Tsigaridis and Kanakidou, 2003), and smog chamber experiments form SOA that is substantially less oxygenated and therefore less hygroscopic than aged atmospheric OAs (Aiken *et al*., 2008). There is growing evidence that these and other atmospheric observations can be explained, at least in part, by multiphase SOA formations involving aqueous reactions in clouds, fog, and wet aerosols. Predictions and experiments by several researchers provide strong support for the following. Alkene and aromatic emissions are oxidized in the gas phase, including in the interstitial spaces of clouds; their water-soluble products partition into atmospheric waters (wet aerosols, clouds, and fog) where they react further, forming low volatility products including organic acids, organosulfates, and oligomers; after water evaporation these products remain in the particle phase, at least in part, forming SOA. The SOA formed from aqueous reactions is more hygroscopic than smog chamber SOA. It has an O/C ratio similar to that of an aged atmospheric aerosol, and it is formed through precursors that are different from those of the traditional SOA. Thus, adding this process to models increases the atmospheric burden, and the spatial and temporal distribution and properties of the predicted SOA are changed. SOA formation through aqueous chemistry has been included in a few modeling studies. Although the uncertainties are large, these regional (northeastern U.S.) and global CTM studies estimate that SOA formed through aqueous chemistry is comparable in magnitude to that formed through the traditional pathway. Although several types of atmospheric measurements provide evidence for this process, its large predicted impacts on aerosol concentrations (and properties), both regionally and globally, provides strong motivation for comprehensive field studies to seek evidence of this process and provide data for broader scientific use.

In this paper, we summarized the concentrations of atmospheric gaseous VOCs and non-refractory fine particle (PM_1; diameter of particle matter less than 1 μm) compositions including nitrate, sulfate, and organic matter concentrations. Further, new particle formation and growth events are investigated, and the mechanisms of formation of SOA are discussed.

2. METHODS

2.1 Measurement Site

The field measurements were made at the Baengnyeong Island atmospheric research supersite, Korea (37.97°N, 124.63°E, 100 m above sea level), operated by the Korea National Institute of Environmental

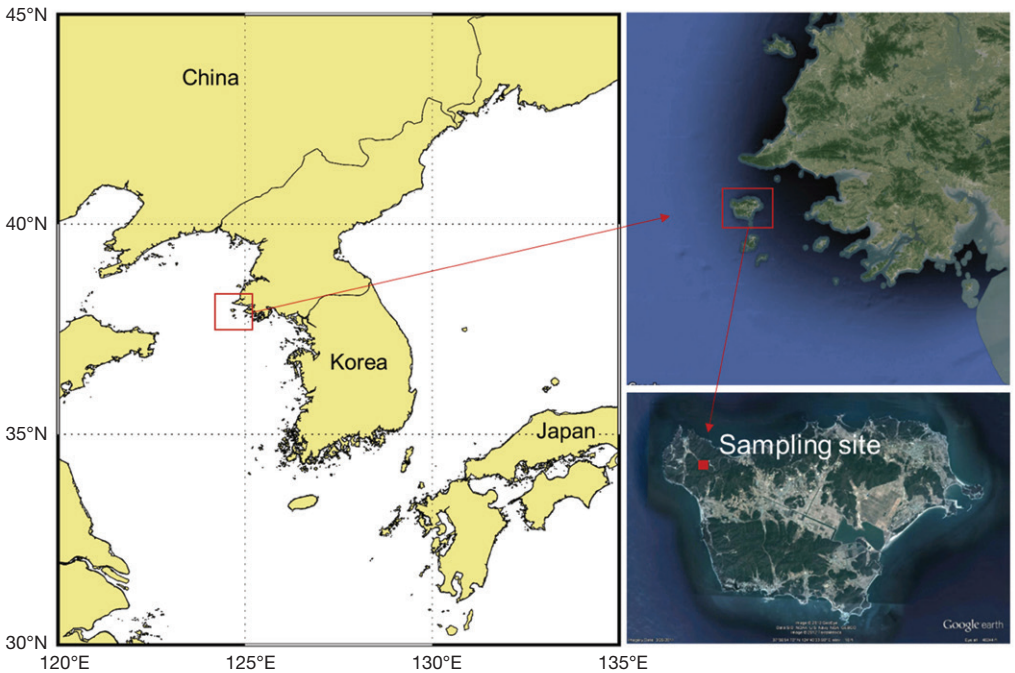

Fig. 1. Map of Korea showing the sampling location at Baengnyeong Island. The satellite images were obtained from google map.

Research (NIER). The supersite is located in between west coast of the Korea, and Shandong Peninsula in eastern China (Fig. 1). The measurement site is suited for monitoring the characteristics of background aerosol level, because it is located at the top of a hill aparted from the island's sparsely populated area. The measurements were conducted from February to November 2012 including an intensive period of September 21 to 29, 2012.

2.2 Instrumentation and Measurement Technique

Non-refractory sub-micron aerosol (PM_1) composition was measured using HR-ToF-AMS. The operation of the Aerodyne HR-ToF-AMS has been described in detail elsewhere (DeCarlo *et al*., 2006; Drewnick *et al*., 2005; Jimenez *et al*., 2003; Jayne *et al*., 2000). Ambient air was drawn through a URG cyclone (D_{50} (mass median diameter) = 2.5 μm, 3 L/min). Perma Pure dryers (MD-110-24, Perma Pure LLC.) were used to control the sample humidity, and the uncertainties from the bounce-related changes in the collection efficiency and the particle transmission through the aerodynamic lens were therefore both reduced. Detailed descriptions and procedures for the calibration of the AMS at Baengnyeong Island atmospheric research supersite are given in Lee *et al*. (2015). In this study, a six-minute time resolution was used to determine the non-refractory fine particle composition, including nitrate, sulfate, ammonium, and organic matter concentrations.

The PTR-ToF-MS was deployed to collect the VOC mixing ratio at the site. The basic principle of this instrument has been described elsewhere in detail (Graus *et al*., 2010; Jordan *et al*., 2009). The gas sample inlet was heated to ~60°C to prevent the wall loss of VOCs. During the intensive period, the drift tube of the PTR-ToF-MS was operated at a temperature of 60°C, a drift voltage of 600 V, and a pressure of ~2.2 hPa, as controlled by software. These conditions correspond to an E/N (electric field to number density of air ratio) value of ~138 Td. Ions were pulsed every 60 μs into the time-of-flight region, and they were detected by the Multi Channel Plate (MCP) at 0.2 ns resolution. Data were stored every one minute in the compressed HDF5 format. The data processing for the determination of the mass calibration, ion fitting (e.g., peak shape, peak height, and peak width), and transmission efficiency by standard gases was carried out according to the Igor routine.

The aerosol number concentrations were measured by using a scanning mobility particle sizer (SMPS, TSI model 3034) with Nafion® dryer. The SMPS was operated with an aerosol flow rate of 1.0 L/min through the Kr-85 neutralizer, and a sheath airflow rate of 5.0 L/min. The size range was set as 10-470 nm for

the mobility diameter, with a measurement interval of 5 minutes. The general principle and operation of the instrument has been described in detail elsewhere (Kim *et al*., 2013; Kulmala *et al*., 2004).

The measurements of gaseous pollutants (O_3, NO_x, CO, and SO_2) were conducted on an hourly basis. The general details for the instrument has been described in Lee *et al*. (2012). The hourly relative humidity data were obtained from an auto weather station (AWS; operated by the Korea Meteorological Administration) at a distance of 0.5 km in a northwest direction.

The NOAA HYSPLIT model (GDAS1) was used to analyze the aerosol composition and the VOC by computing four back-trajectories per day for the air masses arriving at the sampling site with a receptor height of 150 m, which is the same as the height of the site. The back-trajectories were run for 72 hours.

2.3 Positive Matrix Factorization (PMF) Analysis

The timeline of AMS aerosol mass spectra was analyzed using positive matrix factorization (PMF), a multivariate factor analysis tool (Paatero, 1997; Paatero and Tapper, 1994). We used the Igor Pro-based PMF evaluation tool (PET) (Ulbrich *et al*., 2009). PMF was performed upon the V-mode AMS data after applying the error preparations outlined in SQUIRREL and PET. The PMF is described in detail in Lee *et al*., 2015.

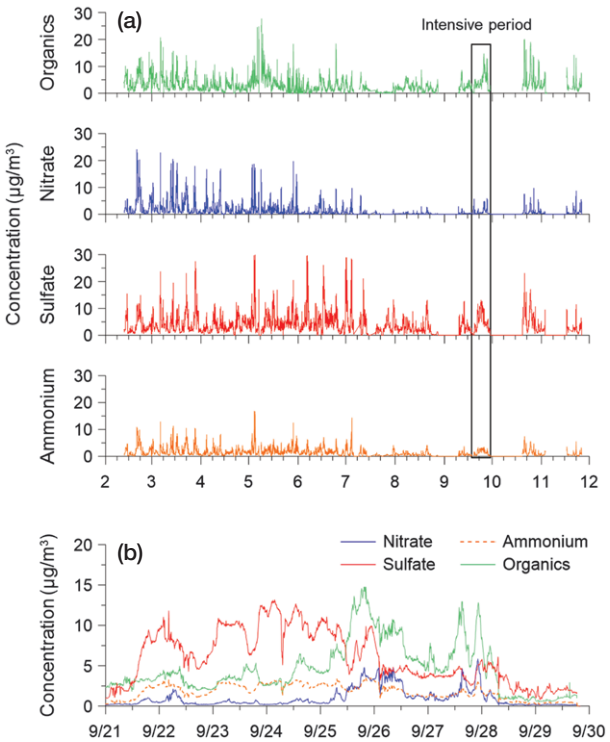

Fig. 2. Timelines of PM_1 organic, ammonium, sulfate, and nitrate concentrations measured using HR-ToF-AMS during: (a) February to November, 2012 and (b) the intensive study period of September 21-29, 2012.

3. RESULTS AND DISCUSSION

3.1 General Characteristics of Submicron Aerosol and Volatile Organic Compounds (VOCs)

Fig. 2a depicts the timelines of the concentrations measured between February and November, 2012, and Fig. 2b presents a time series of the concentrations that were observed during the intensive study period of from September 21th to 29th, 2012. Organic matter and sulfate were generally the most abundant aerosol components, and they exhibited maximum concentrations of 30 μg/m^3 and 29 μg/m^3, respectively (Fig. 2a). The nitrate concentrations peaked at 25 μg/m^3, but they were typically much lower than the sulfate and organic matter concentrations. The period from February to June and October featured the higher concentrations of the organics, nitrate, and sulfate, with the lower concentrations observed from July through September due to the relatively clean air masses that generally reach the site during those months of the year (Lee *et al*., 2015). Another interesting observation is the variation of the nitrate concentration at the site according to the different months. Nitrate reached a low concentration when the temperature reached a maximum in the summer time period of July to October, supporting the theory that temperature has an impact on the gas-particle partitioning of nitric acid and NH_4NO_3 dissociation (Lee *et al*., 2008a, b; Yu *et al*., 2006).

Mass peaks with signals above the noise were identified, and include major primary ions (e.g. $(H_2O)H^+$, $(H_2O)_2H^+$, and water clusters), impurities such as O_2^+ and NO_2^+, and ammonium ions. In this paper, we focus on the 17 selected ion species shown in Fig. 3. The detectable biogenic VOCs (BVOCs) from the site were isoprene (*m/z* 69.071), 2-methyl-3-buten-2-ol (MBO, *m/z* 87.077), dimethyl sulfide (DMS, *m/z* 63.071), and monoterpenes (*m/z* 81.070, 95.086, 137.131), with the averaged mixing ratios of 0.24 ppbv, 0.25 ppbv, 0.20 ppbv, and 0.38 ppbv during the intensive study period, respectively. Toluene (*m/z* 135.116, 0.45 ppb) and benzene (*m/z* 79.054, 0.32 ppb) comprised the majority of the anthropogenic VOCs (AVOCs) with the averaged mixing ratios of 0.45 ppb and 0.32 ppb during the intensive study period of September 23 to 29, respectively. For the oxygenated VOCs (OVOCs), acetone (*m/z* 59.048), acetaldehyde

(*m/z* 45.033), acetic acid (*m/z* 61.027), formic acid (*m/z* 46.997), and methyl vinyl ketone and methacrolein (MVK + MACR, *m/z* 71.048) were measured.

MVK + MACR are well known major secondary products from the atmospheric oxidation of isoprene. The mixing ratio of MVK + MACR was measured between 0.01 and 1.81 ppbv at the site. Acetone is ubiquitous in the atmosphere and has a variety of sources including terrestrial vegetation, anthropogenic emissions, and photochemical productions. Acetone was the most abundant VOC with an average of approximately 4 ppbv, but its range is from 0.96 to 17.53 ppbv, which is very similar to the ranges found in previous studies (Park *et al*., 2013; Yuan *et al*., 2013). Acetaldehyde is emitted by live leaves, and its sources are similar to acetone. The acetaldehyde was measured with an average of 2.67 ppbv with mixing ratios between 1.09 and 12.48 ppbv. Acetic acid was among the top three measured species with mixing ratios ranging from 0.01 to 28.34 ppbv, and an average of 1.67 ppbv. OVOC may be a result of the oxidation processes of BVOC and AVOC in the atmosphere. Acetone, acetaldehyde, acetic acid, and formic acid were measured for approximately 74% of the total measured VOCs, suggesting strong oxidation processes at the site (Fig. 3).

The total BVOCs shown in the lower panel of Fig. 4 include isoprene, MBO, DMS, and monoterpenes.

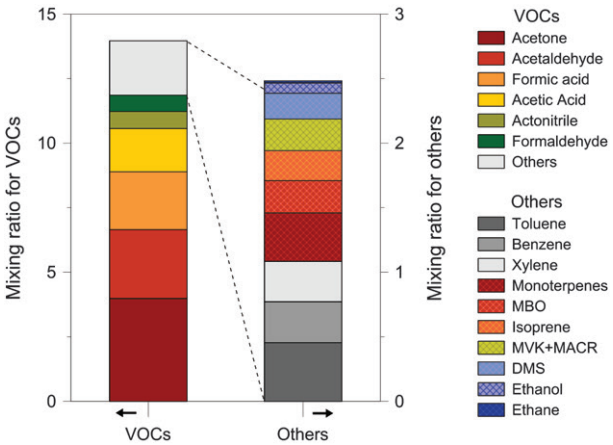

Fig. 3. Averaged mixing ratios (labels in each bar) for 17 selected ion species during the intensive study period of September 23-29, 2012.

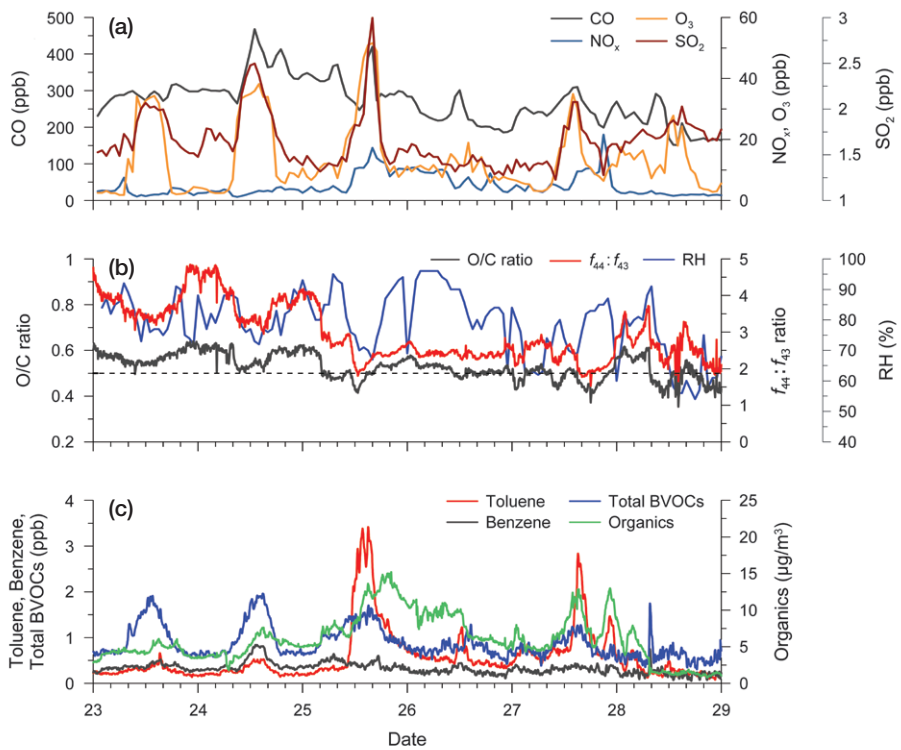

Fig. 4. Timelines of the intensive study period of 9/23-29, 2012 of gaseous pollutants (CO, NO_x, O_3, and SO_2; upper panel); O/C, $f_{44}:f_{43}$ ratios for PTR-ToF-MS and relative humidity (middle panel); and major anthropogenic VOCs (toluene and benzene and total biogenic VOCs) and organics (bottom panel) (Note: (a) aqSOA formation, (b) gasSOA formation, and (c) nighttime aqSOA).

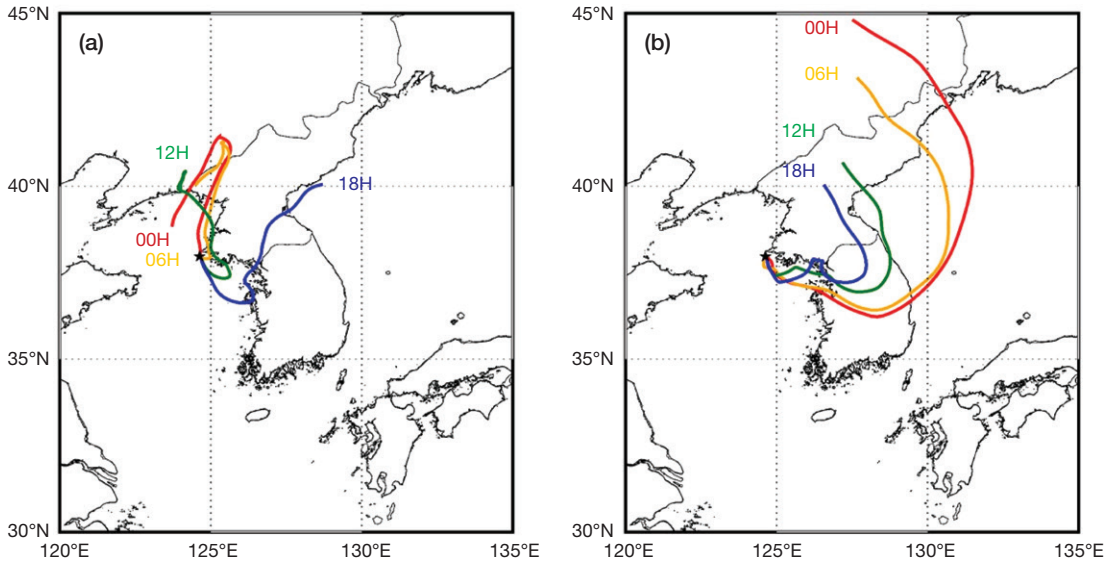

Fig. 5. Back trajectories of air masses arriving at Baengnyeong Island for (a) 9/25 and (b) 9/27, 2012.

MBO is emitted from certain pine trees (Holzinger *et al*., 2005). Isoprene, MBO, and monoterpenes were measured for approximately 7.4% of the total measured VOCs (Fig. 3). The measured BVOCs showed that emissions were at a maximum during the daytime around 14:00 local time (Fig. 4). The highest concentrations of BVOCs were observed at the beginning of the intensive study period with a maximum of ~2 ppbv, and with concentrations decreasing to 0.5 ppbv at the end of the study (Fig. 4).

The highest concentrations of toluene were observed from September 25 to 27 when concentrations of BVOCs were low. In general, benzene was measured at low concentrations, with a maximum of 0.89 ppbv during the entire intensive study period. The AVOCs (toluene and benzene) were measured for approximately 5.4% of the total measured VOCs. Fig. 4 demonstrates an interesting relationship between toluene and benzene. Benzene is predominantly derived more from vehicles, and it is well-correlated with other aromatic VOCs such as toluene when the main source of aromatic VOCs is vehicle exhausts. The benzene concentration trends were similar to those of toluene on September 23 to 24, indicating that toluene and benzene may be derived from the same source, as follows: local motor vehicle exhausts. Periods of relatively high toluene concentrations were, however, observed on September 25 and 27 along with the lowest concentrations of the benzene. This is associated with the transport of polluted air masses to the site, as shown Fig. 5. The air mass trajectories in Fig. 5 show that air masses on September 27 spent time over industrial areas in Korea before arriving at the site, while air masses passed over China until 12:00 LST on September 25, when the high concentration of toluene was observed.

3.2 Determination of Secondary Organic Aerosol Formation Mechanisms

It is well accepted that SOA forms through the partitioning of semivolatile products of the gas-phase photochemical reactions of VOCs and atmospheric oxidants (Pankow, 1994a, b). This process has been studied extensively in smog chambers. According to partitioning theory, the major factors are considered to be the volatility of gas-phase oxidation products, the organic mass in the pre-existing particles, and temperature. Precursors must be large ($>C_7$) to produce high SOA yields, because they must produce products with low enough volatility to partition substantially into the organic matter in the particle phase. Because precursors are large and only a few oxidation steps are needed to form condensable products, the O/C ratio of "smog-chamber" SOA is modest (0.3 to 0.4; Aiken *et al*., 2008). Higher SOA yields typically occur in lower NO experiments (higher VOC/NO), because the products from high NO are smaller and more volatile. Partitioning theory is a fundamental tool in the modeling of SOA (Donahue *et al*., 2006; Odum *et al*., 1996; Pankow, 1994a, b).

While clearly important, it fails to consider that, in many locations, the liquid water in aerosols, clouds, and fog may be a more accessible medium than organic matter for the partitioning of gas-phase oxidation products (Turpin *et al*., 2000). Lim *et al*. (2013) explained that glyocal (C_2), methyglyoxal (C_3), and acetic acid have great potential to form SOA via aqueous chemis-

try in clouds, fogs, and wet aerosols. For aqueous SOA (aqSOA) formation to be substantial, the precursor compounds must be highly water soluble. This suggests that aqSOA will have high polarity and O/C ratios (O/C) = 1-2, 1.5, and 2 for glyoxal, methyglyoxal, and oxalate, respectively, and O/C = ~1 at aerosol relevant concentrations (Perri *et al*., 2009; Altieri *et al*., 2008).

To gain further insight into the mechanisms of formation of the SOA at the Baengnyeong Island sampling site, several cases were considered. Fig. 4 also shows the timelines of the gaseous pollutants, and the relationship of the O/C and $f_{44}:f_{43}$ ratios with precursor VOCs and OAs during the intensive study period. The values of $f_{44}:f_{43}$ describe ambient OA oxidation. The relative abundances of the key OA ions at *m/z* 44 (CO_2^+) and *m/z* 43 ($C_2H_3O^+$) distinguish the semi-volatile oxygenated OA (SV-OOA) from the low volatility oxygenated OA (LV-OOA). The low $f_{44}:f_{43}$ values ($\leq$ ~1) suggest that the bulk of the observed OA is slightly aged/oxidized, and likely resembles the previously reported SV-OOA from the SOA formation chamber studies for relatively fresh aerosol, whereas the high $f_{44}:f_{43}$ values indicate that the OA is very oxidized or very similar to previously reported reference spectra of POA emitted directly from anthropogenic sources. The timeline of the $f_{44}:f_{43}$ ratio shows that the observed OA was relatively oxidized from September 23 to 25, while the OAs was more likely to be fresh aerosol in SOA. The ratios of O/C and $f_{44}:f_{43}$ decreased with the increasing availability of the precursor BVOCs and AVOCs. Different chemical pathways have been proposed here for the mechanisms of formation of SOA based on the O/C ratio described by Ervans *et al*. (2011). In this study, the aqSOA formation was investigated during both the daytime and the nighttime, as in cases (a) and (c), respectively, and the SOA that was formed in the gas phase and was then partitioned to an organic phase (gasSOA) was also examined, as in case (b) (Fig. 4). Cases (a) and (c) showed an aqSOA formation with an O/C ratio of more than 0.5 when a high concentration of VOCs (BVOCs and AVOCs) is present. On the other hand, the O/C ratio of less than 0.5 in case (b) suggests a possible mechanism of gasSOA formation. The time series of the relative humidity during the intensive study period did not, however, show a significant variation, except during the last gasSOA episode (after September 28, 12:00). The mean relative humidity of the aqSOA and gasSOA episodes were 78.7% and 73%, respectively, which were relatively high due to the geographical location. Compared with the aqSOA episode, the gaseous pollutants (especially SO_2 and O_3) and the toluene rapidly increased during the gasSOA episode. It can therefore be easily deducted that Baengnyeong Island was dominated by aqSOA due to a high relative humidity, except when the gaseous pollutants and VOCs (especially toluene) increased to cause the formation of gasSOA.

3. 3 Positive Matrix Factorization (PMF) Analysis of AMS Data Set

To identify the reasonable factors, the oxygenated OA (OOA) components in the triangle plot are transformed into the Van Krevelen diagram, which can indicate bulk changes in oxygenation in ambient datasets, and it may also be used to explore the reaction mechanisms in isolated airmasses (Fig. 6a). The data

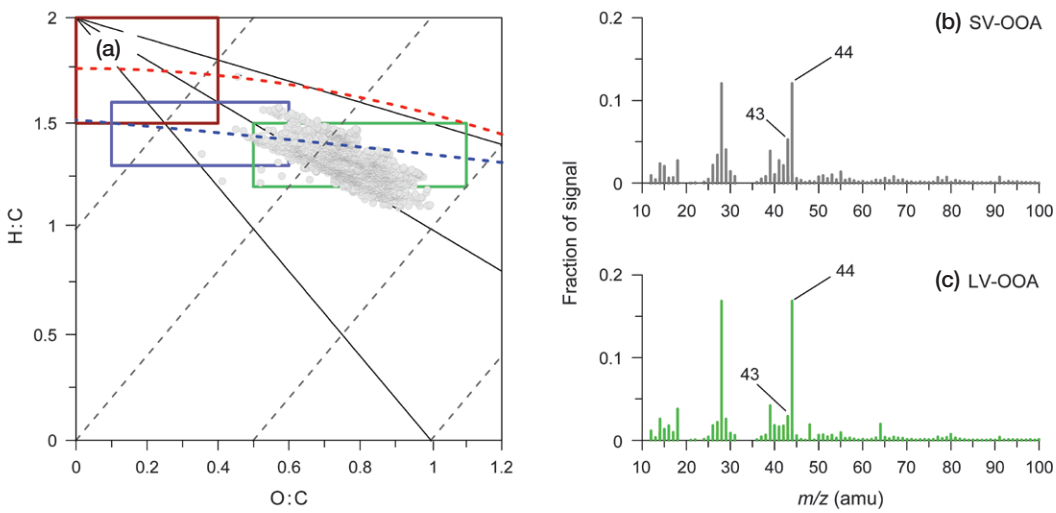

Fig. 6. (a) Van Krevelen -triangle diagram for the OA components from the organics with HR-AMS data. The mass spectra of the two OA factors ((b) SV-OOA and (c) LV-OOA) were determined on the basis of PMF analysis of the HR-AMS data from September 2012.

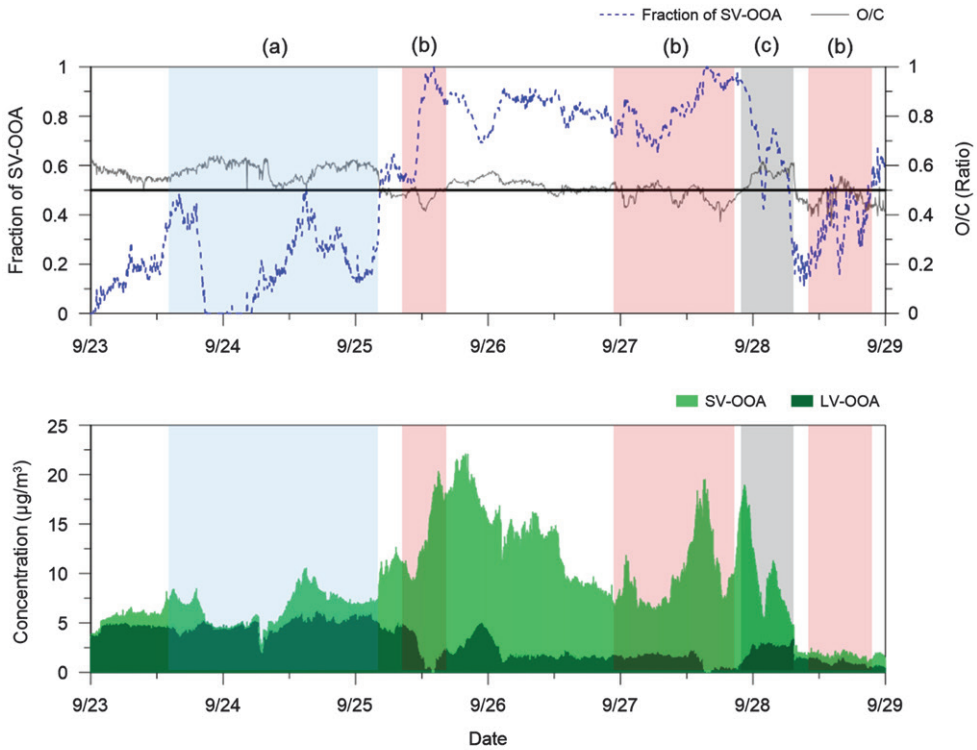

Fig. 7. Time series of fractions of SV-OOA and O/C ratio (upper) and SV-OOA and LV-OOA (bottom) during the intensive measurement period (Note: (a) aqSOA formation, (b) gasSOA formation, and (c) nighttime aqSOA).

points in the apex of the triangle area (higher O : C and lower H : C) indicates highly oxidized particles on the van Krevelen-triangle diagram (Ng *et al*., 2011). The SV-OOA located in 1.3-1.6 for H : C and 0.1-0.6 for O : C, whereas the LV-OOA is more oxidized, with lower H : C than SV-OOA at 1.2-1.5 (Aiken *et al*., 2008, 2007). Therefore, we concluded that there is no POA from the intensive period of this study, and it would be reasonable to divide into the two factors of SV-OOA and LV-OOA.

The results from the PMF analysis of AMS observations consequently yielded the two factors of SV-OOA (46% of OM) and LV-OOA (54% of OM). Both SV-OOA and LV-OOA were indicated by a higher signal at *m/z* 44 (CO_2) than *m/z* 43 ($C_3H_7^+$ and $CH_3CO_3^+$), whereas an LV-OOA that is highly oxidized has a more dominant peak at *m/z* 44 than SV-OOA. The LV-OOA factor has a fractional *m/z* 44 (f_{44}) of 17% and a fractional *m/z* 43 (f_{43}) of 3%, similar to the typical LV-OOA factors that are based on the aerosol volatility (f_{44} = 12-15%, f_{43} = 5-7%) determined in previous studies (Ng *et al*., 2011, 2010; Zhang *et al*., 2011; Hildebrandt *et al*., 2010). The SV-OOA factor is distinguished by a much lower fraction of *m/z* 44 (f_{44} = 12%) than seen in LV-OOA, indicating less oxidized (Ng *et al*., 2011). Typically, SV-OOA and LV-OOA have characteristics that are well correlated with nitrate and sulfate, respectively (Zhang *et al*., 2011). Indeed, the two factors were highly correlated with nitrate and sulfate, with high correlation coefficients of 0.93 and 0.91, respectively, according to the AMS (not shown).

Fig. 7 shows the time series of the fraction for SV-OOA, and the O/C ratios and concentrations of SV-OOA and LV-OOA during the intensive measurement period. The thresholds of the O/C ratio (0.5) for the distinguished gasSOA and aqSOA, and the negative correlation shown by the fraction of the SV-OOA (R = ~ −0.55) with the O/C ratio all need to be considered here. It should also be noted that the fraction of SV-OOA in the aqSOA was relatively low compared with that in the gasSOA, whereas the fraction of SV-OOA rapidly increased in the gasSOA, especially in the first and second gasSOA periods, when the concentrations of toluene, benzene, and total BVOC was highest during the intensive period. For SV-OOA, the highest concentrations were indicated during the first and second gasSOA periods. The fraction and concentration of SV-OOA then significantly decreased for the nighttime aqSOA. However, the third gasSOA period showed an increase in the fraction of SV-OOA. Though aqSOA was dominant at Baengnyoung Island, this phenomenon can be interpreted as the activation of gasSOA by

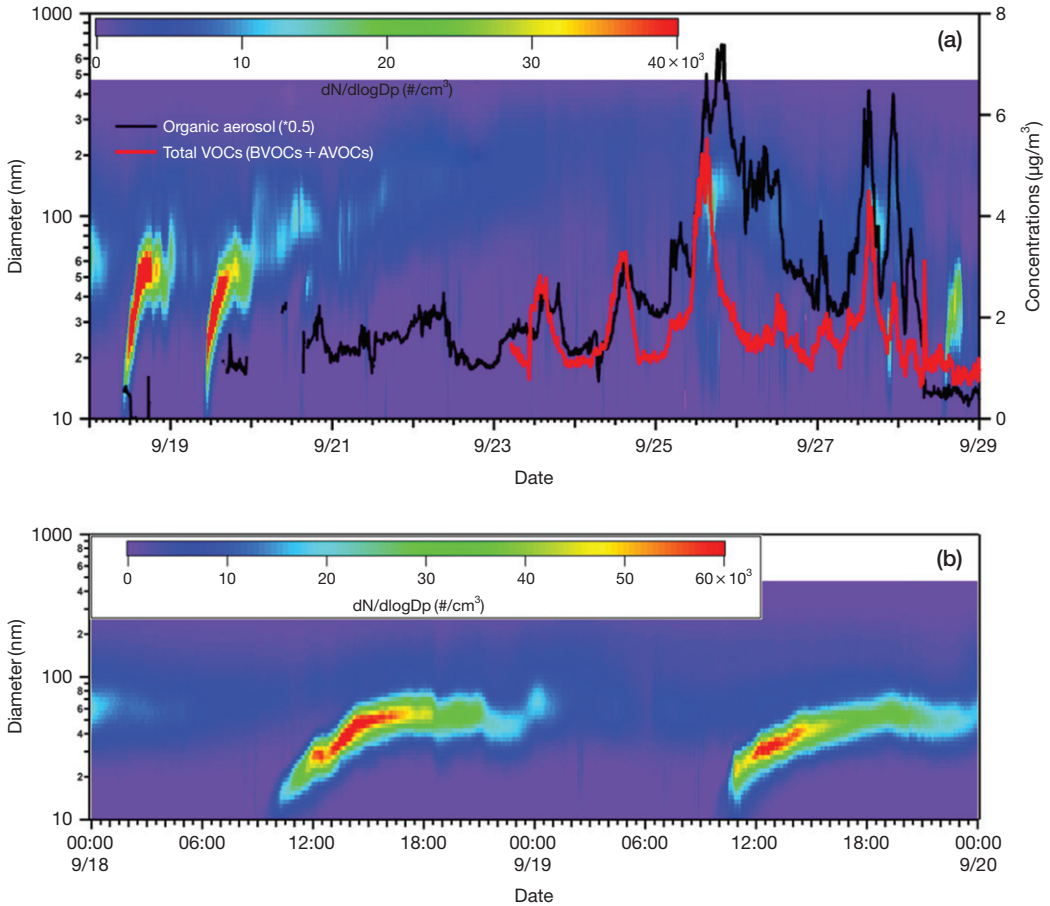

Fig. 8. (a) Time series of aerosol number distribution by SMPS, and concentrations of organic and total VOCs (biogenic VOCs + anthropogenic VOCs) measured by HR-ToF-AMS and PTR-ToF-MS, respectively, at Baengnyeong Island, and (b) aerosol number distribution evolution during a new particle formation event.

gaseous pollutants and VOCs, resulting in an increase of SV-OOA.

3.4 Observation of New Particle Formation

During the intensive period, we observed several days (September 18 and 19) of increases in number concentrations of the smallest measured particles, along with a succeeding development of the aerosol size distribution (Fig. 8a). It is similar to the new particle formation (NPF) events shown in previous studies (Kim *et al*., 2013; Levin *et al*., 2012; Boy *et al*., 2008; Kulmala *et al*., 2004). Boy *et al*. (2008) divided the events according to nucleation and growth. For the NPF events, nucleation mode particles (3-10 nm) were clearly observed at the event, while new particle formation events (particles smaller than 6 nm) were not observed. They explained that the nucleation started upwind with a subsequent particle growth as the aerosol population was transported the site. Even though our measurements do not extend to particles smaller than 10 nm, there was no significant extension of the particle number distribution around 10 nm, as shown in Fig. 8b. The events on September 18 and 19 are more likely to be "new particle formation". The previous studies often observed NPF under high concentrations of gaseous VOCs. However, our measurements showed that there was no new particle formation during the times of high concentrations of gaseous VOCs on September 25 and 27 (Fig. 8a). This supports that gas to particle conversion by absorption and adsorption involves interaction of the gaseous VOCs with the pre-existing aerosol particles in polluted conditions. Because concentrations of the VOCs from the PTR-ToF-MS are not available, NPF on September 18 and 19 cannot be clearly explained. However, a back-trajectory analysis shows that the air masses that arrived on September 18 and 19 passed through the relatively clean environment of the northern parts of China and Korea (Fig. 9a and 9b), while the air mass of September 28 passed through relatively polluted regions (Fig.

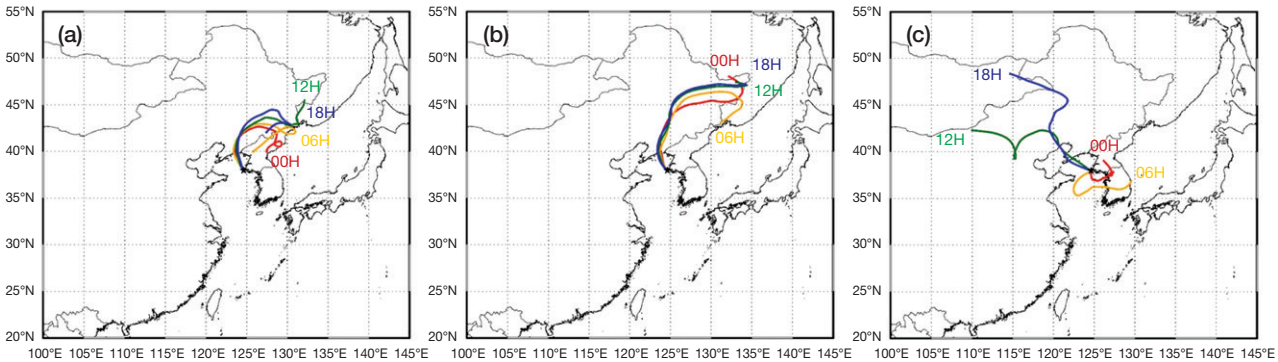

Fig. 9. Back trajectories of air masses arriving at Baengnyeong Island for (a) 9/18, (b) 9/19, and (c) 9/28, 2012.

9c), and a high population of large size particles (~30 nm) was observed (Fig. 8a). It was hypothesized that the NPF began upwind with the subsequent growth as the aerosol population was transported to the site from the ocean, and that a clean condition is very important for the NPF at this site.

4. SUMMARY AND CONCLUSIONS

The chemical composition of non-refractory submicron particles (PM_1) was measured at an air quality supersite on Baengnyeong Island during the period from February to November 2012, and VOCs including BVOC, OVOC and AVOCs were also measured during an intensive study period from September 23 to 29 using PTR-ToF-MS. The mixing ratio of MVK + MACR was measured in a range of 0.01-1.81 ppbv at the site, and the average mixing ratios of the acetone and acetaldehyde are ~4 ppbv and 2.67 ppbv, respectively. The OVOCs except MVK + MACR were measured for ~74% of total measured VOCs, suggesting the occurrence of strong oxidation processes at the site. The total BVOCs including isoprene, MBO, DMS, and monoterpenes were measured for 7.4% of total measured VOCs, and the maximum emissions occurred during the daytime at around 14:00 local time. The highest concentrations of toluene were observed from September 25 to 27 during periods of low BVOC and benzene concentrations, indicating an association with the transport of polluted air masses to the site.

The observed OA was relatively oxidized from September 23 to 25, with the OAbeing more likely to be fresh aerosol in SOA formation. This might be caused by the different chemical pathways in the mechanisms of formation of SOA based on the O/C ratio, which is shown by the aqueous SOA (aqSOA) formation during both the daytime and the nighttime. It was also formed in the gas phase, and it then partitioned to an organic phase (gasSOA). The aqSOA formation showed an O/C ratio that is more than 0.5 when a high concentration of VOCs (BVOCs and AVOCs) was present. On the other hand, an O/C ratio of less than 0.5 suggests that gasSOA formation is a possible mechanism. Since the relative humidity values of the aqSOA and gasSOA did not show any significant difference, the concentrations of the gaseous pollutants and VOCs could be a main driver in the determination of aqSOA or gasSOA formations under high relative humidity conditions at Baengnyeong Island. Moreover, the concentration and fraction of SV-OOA was significantly increased in the gasSOA when the concentrations of the gaseous pollutants and VOCs were high.

In relation to the "new particle formation" events (September 18 and 19), particles smaller than 6 nm were not observed, but nucleation mode particles (3-10 nm) and particles of more than 6 nm were observed. This could be explained if the nucleation started upwind with the subsequent particle growth as the aerosol population was transported to the site, although our measurements do not extend to particles smaller than 10 nm. There was no new particle formation during the times of high concentrations of gaseous VOCs on September 25 and 27, which might be an effect of the gas to particle conversion by absorption and adsorption that involves the interaction of the gaseous VOCs with the pre-existing aerosol particles under a polluted condition. It was hypothesized that the new particle formation began upwind with the subsequent growth as the aerosol population was transported to the site from the ocean, indicating that a clean condition is very important for new particle formation at this site.

ACKNOWLEDGEMENTS

The authors thank the research scientists at Baengnyeong Island and the Climate & Air Quality Research

Department at the National Institute of Environmental Research (Korea) for their contributions to the success of the field campaign. The data analysis and additional data processing were supported by a Grant from the National Research Foundation of Korea (NRF-2014R1 A1A1007947) and the additional data processing were supported by Hankuk University of Foreign Studies Research Fund (2017045001).

REFERENCES

Aiken, A.C., DeCarlo, P.F., Jimenez, J.L. (2007) Elemental analysis of organic species with electron ionization high-resolution mass spectrometry. Analytical Chemistry 79, 8350-8358.

Aiken, A.C., DeCarlo, P.F., Kroll, J.H., Worsnop, D.R., Huffman, J.A., Docherty, K., Ulbrich, I.M., Mohr, C., Kimmel, J.R., Sueper, D., Zhang, Q., Sun, Y., Trimborn, A., Northway, M., Ziemann, P.J., Canagaratna, M.R., Onasch, T.B., Alfarra, R., Prevot, A.S.H., Dommen, J., Duplissy, J., Metzger, A., Baltensperger, U., Jimenez, J.L. (2008) O/C and OM/OC ratios of primary, secondary, and ambient organic aerosols with high resolution time-of-flight aerosol mass spectrometry. Environmental Science & Technology 42, 4478-4485.

Altieri, K.E., Seitzinger, S.P., Carlton, A.G., Turpin, B.J., Klein, G.C., Marshall, A.G. (2008) Oligomers formed through in-cloud methylglyoxal reactions: Chemical composition, properties, and mechanisms investigated by ultra-high resolution FT-ICR mass spectrometry. Atmospheric Environment 42, 1476-1490.

Andrews, E., Saxena, P., Musarra, S., Hildemann, L.M., Koutrakis, P., McMurry, P.H., Olmez, I., White, W.H. (2000) Concentration and composition of atmospheric aerosols from the 1995 SEAVS experiment and a review of the closure between chemical and gravimetric measurements. Journal of Air & Waste Management Association 50, 648-664.

Boy, M., Karl, T., Turnipseed, A., Mauldin, R.L., Kosciuch, E., Greenberg, J., Rathbone, J., Smith, J., Held, A., Barsanti, K., Wehner, B., Bauer, S., Wiedensohler, A., Bonn, B., Kulmala, M., Guenther, A. (2008) New particle formation in the Front Range of the Colorado Rocky Mountains. Atmospheric Chemistry and Physics 8, 1577-1590.

Charlson, R.J., Schwartz, S.E., Hales, J.M., Cess, R.D., Coakley, J.A., Hansen, J.E., Hofmann, D.J. (1992) Climate Forcing by Anthropogenic Aerosols. Science 255, 423-430.

Chow, J.C., Watson, J.G., Fujita, E.M., Lu, Z.Q., Lawson, D.R., Ashbaugh, L.L. (1994) Temporal and Spatial variations of $PM_{2.5}$ and PM_{10} aerosol in the outhern California Air-Quality study. Atmospheric Environment 28, 2061-2080.

Chung, S.H., Seinfeld, J.H. (2002) Global distribution and climate forcing of carbonaceous aerosols. Journal of Geophysical Research 107, doi:10.1029/2001JD 001397

Corrigan, C.E., Novakov, T. (1999) Cloud condensation nucleus activity of organic compounds: a laboratory study. Atmospheric Environment 33, 2661-2668.

DeCarlo, P.F., Kimmel, J.R., Trimborn, A., Northway, M.J., Jayne, J.T., Aiken, A.C., Gonin, M., Fuhrer, K., Horvath, T., Docherty, K.S., Worsnop, D.R. Jimenez, J.L. (2006) Field-deployable, high-resolution, time-of-flight aerosol mass spectrometer. Analytical Chemistry 78, 8281-8289.

Donahue, N.M., Robinson, A.L., Stanier, C.O., Pandis, S.N. (2006) Coupled partitioning, dilution and chemical aging of semivolatile organics. Environmental Science and Technology 40, 2635-2643.

Donahue, N.M., Robinson, A.L., Pandis, S.N. (2009) Atmospheric organic particulate matter: From smoke to secondary organic aerosol. Atmospheric Environment 43, 94-106.

Drewnick, F., Hings, S.S., DeCarlo, P., Jayne, J. T., Gonin, M., Fuhrer, K., Weimer, S., Jimenez, J. L., Demerjian, K.L., Borrmann, S., Worsnop, D.R. (2005) A new time-of-flight aerosol mass spectrometer (TOF-AMS)–instrument description and first field deployment. Aerosol Science and Technology 39, 637-658.

Ervans, B., Turpin, B.J., Weber, R.J. (2011) Secondary aerosol formation in cloud droplets and aqueous particles (aqSOA): a review of laboratory, field and model studies. Atmospheric Chemistry and Physics 11, 11069-11102.

Fuzzi, S., Andreae, M.O., Huebert, B.J., Kulmala, M., Bond, T.C., Boy, M., Doherty, S.J., Guenther, A., Kanakidou, M., Kawamura, K., Kerminen, V.M., Lohmann, U., Russell, L.M., Poschl, U. (2006) Critical assessment of the current state of scientific knowledge, terminology, and research needs concerning the role of organic aerosols in the atmosphere, climate, and global change. Atmospheric Chemistry and Physics 6, 2017-2038.

Giebl, H., Berner, A., Reischl, G., Puxbaum, H., Kasper-Giebl, A., Hitzenberger, R. (2002) CCN activation of oxalic and malonic acid test aerosols with the University of Vienna cloud condensation nuclei counter. Journal of Aerosol Science 33, 1623-1634.

Graus, M., Müller, M., Hansel, A. (2010) High Resolution PTR-TOF: Quantification and Formula Confirmation of VOC in Real Time. Journal of the American Society for Mass Spectrometry 21, 1037-1044.

Heald, C.L., Jacob, D.J., Park, R.J., Russell, L.M., Huebert, B.J., Seinfeld, J.H., Liao, H., Weber, R.J. (2005) A large organic aerosol source in the free troposphere missing from current models. Geophysical Research Letters 32, doi:10.1029/2005GL023831

Hildebrandt, L., Engelhart, G.J., Mohr, C., Kostenidou, E., Lanz, V.A., Bougiatioti, A., DeCarlo, P.F., Prevot, A.S.H., Baltensperger, U., Mihalopoulos, N., Donahue, N.M., Pandis, S.N. (2010) Aged organic aerosol in the Eastern Mediterranean: The Finokalia Aerosol Mea-

surement Experiment-2008. Atmospheric Chemistry and Physics 10, 4167-4186.
Holzinger, R., Lee, A., Paw, K.T., Goldstein, A.H. (2005) Observations of oxidation products above a forest imply biogenic emissions of very reactive compounds. Atmospheric Chemistry and Physics 5, 67-75.
Hoyle, C.R., Berntsen, T., Myhre, G., Isaksen, I.S.A. (2007) Secondary organic aerosol in the global aerosol - chemical transport model Oslo CTM2. Atmospheric Chemistry and Physics 7, 5675-5694.
Huffman, J.A., Docherty, K.S., Mohr, C., Cubison, M.J., Ulbrich, I.M., Ziemann, P.J., Onasch, T.B., Jimenez, J.L. (2009) Chemically-Resolved Volatility Measurements of Organic Aerosol from Different Sources. Environmental Science and Technology 43, 5351-5357.
Jayne, J.T., Leard, D.C., Zhang, X.F., Davidovits, P., Smith, K.A., Kolb, C.E., Worsnop, D.R. (2000) Development of an aerosol mass spectrometer for size and composition analysis of submicron particles. Aerosol Science and Technology 33, 49-70.
Jimenez, J.L., Canagaratna, M.R., Donahue, N.M., Prevot, A.S.H., Zhang, Q., Kroll, J.H., DeCarlo, P.F., Allan, J.D., Coe, H., Ng, N.L., Aiken, A.C., Docherty, K.S., Ulbrich, I.M., Grieshop, A.P., Robinson, A.L., Duplissy, J., Smith, J.D., Wilson, K.R., Lanz, V.A., Hueglin, C., Sun, Y.L., Tian, J., Laaksonen, A., Raatikainen, T., Rautiainen, J., Vaattovaara, P., Ehn, M., Kulmala, M., Tomlinson, J.M., Collins, D.R., Cubison, M.J., Dunlea, E.J., Huffman, J.A., Onasch, T.B., Alfarra, M.R., Williams, P.I., Bower, K., Kondo, Y., Schneider, J., Drewnick, F., Borrmann, S., Weimer, S., Demerjian, K., Salcedo, D., Cottrell, L., Griffin, R., Takami, A., Miyoshi, T., Hatakeyama, S., Shimono, A., Sun, J.Y., Zhang, Y.M., Dzepina, K., Kimmel, J.R., Sueper, D., Jayne, J.T., Herndon, S.C., Trimborn, A.M., Williams, L.R., Wood, E.C., Middlebrook, A.M., Kolb, C.E., Baltensperger, U., Worsnop, D.R. (2009) Evolution of Organic Aerosols in the Atmosphere. Science 326, 1525-1529.
Jimenez, J.L., Jayne, J.T., Shi, Q., Kolb, C.E., Worsnop, D.R., Yourshaw, I., Seinfeld, J.H., Flagan, R.C., Zhang, X.F., Smith, K.A., Morris, J.W., Davidovits, P. (2003) Ambient aerosol sampling using the Aerodyne Aerosol Mass Spectrometer. Journal of Geophysical Research 108, doi:10.1029/2001JD001213
Jordan, A., Haidacher, S., Hanel, G., Hartungen, E., Märk, L., Seehauser, H., Schottkowsky, R., Sulzer, P., Märk, T.D. (2009) A high resolution and high sensitivity proton-transfer-reaction time-of-flight mass spectrometer (PTR-TOF-MS). International Journal of Mass Spectrometry 286, 122-128.
Kim, Y., Yoon, S., Kim, S., Kim, K., Lim, H., Ryu, J. (2013) Observation of new particle formation and growth events in Asian continental outflow. Atmospheric Environment 64, 160-168.
Kulmala, M., Vehkamäki, H., Petäjä, T., Dal Maso, M., Lauri, A., Kerminen, V.M., Birmili, W., McMurry, P.H. (2004) Formation and growth rates of ultrafine atmospheric particles: a review of observations. Journal of Aerosol Science 35, 143-176.
Kumar, P.P., Broekhuizen, K., Abbatt, J.P.D. (2003) Organic acids as cloud condensation nuclei: Laboratory studies of highly soluble and insoluble species. Atmospheric Chemistry and Physics 3, 509-520.
Lee, G., Choi, H.-S., Lee, T., Choi, J., Park, J.S., Ahn, J.Y. (2012) Variations of regional background peroxyacetyl nitrate in marine boundary layer over Baengyeong Island, South Korea. Atmospheric Environment 61, 533-541.
Lee, T., Choi, J., Lee, G., Ahn, J.Y., Park, J.S., Atwood, S.A., Schurman, M., Choi, Y., Chung, Y., Collett, J.L., Jr. (2015) Characterization of Aerosol Composition, Concentrations, and Sources at Baengnyeong Island, Korea using an Aerosol Mass Spectrometer. Atmospheric Environment 120, 297-306.
Lee, T., Yu, X., Ayres, B., Kreidenweis, S.M., Malm, W.C., Collett, J.L., Jr. (2008a) Observations of fine and coarse particle nitrate at several rural locations in the United States. Atmospheric Environment 42, 2720-2732.
Lee, T., Yu, X., Kreidenweis, S.M., Malm, W.C., Collett, J.L., Jr. (2008b) Semi-continuous measurement of $PM_{2.5}$ ionic composition at several rural locations in the United States. Atmospheric Environment 42, 6655-6669.
Levin, E.J., Prenni, A.J., Petters, M.D., Kreidenweis, S.M., Sullivan, R.C., Atwood, S.A., Ortega, J., DeMott, P.J., Smith, J.N. (2012) An annual cycle of size-resovled aerosol hygroscopicity at a forested site in Colorado. Journal of Geophysical Research 117, doi:10.1029/2011JD016854
Lim, Y.B., Tan, Y., Turpin, B.J. (2013) Chemical insights, explicit chemistry, and yields of secondary organic aerosol from OH radical oxidation of methylglyoxal and glyoxal in the aqueous phase. Atmospheric Chemistry and Physics 13, 8651-8667.
Matsui, H., Koike, M., Takegawa, N., Kondo, Y., Griffin, R.J., Miyazaki, Y., Yokouchi, Y., Ohara, T. (2009) Secondary organic aerosol formation in urban air: Temporal variations and possible contributions from unidentified hydrocarbons. Journal of Geophysical Research 114, doi:0.1029/2008JD010164
Ng, N.L., Canagaratna, M.R., Jimenez, J.L., Chhabra, P.S., Seinfeld, J.H., Worsnop, D.R. (2011) Changes in organic aerosol composition with aging inferred from aerosol mass spectra. Atmospheric Chemistry and Physics 11, 6465-6474.
Ng, N.L., Canagaratna, M.R., Zhang, Q., Jimenez, J.L., Tian, J., Ulbrich, I.M., Kroll, J.H., Docherty, K.S., Chhabra, P.S., Bahreini, R., Murphy, S.M., Seinfeld, J.H., Hildebrandt, L., Donahue, N.M., DeCarlo, P.F., Lanz, V.A., Prevot, A.S.H., Dinar, E., Rudich, Y., Worsnop, D.R. (2010) Organic aerosol components observed in Northern Hemispheric datasets from Aerosol Mass Spectrometry. Atmospheric Chemistry and Physics 10, 4625-4641.

Odum, J.R., Hoffmann, T., Bowman, F., Collins, D., Flagan, R.C., Seinfeld, J.H. (1996) Gas/particle partitioning and secondary organic aerosol yields. Environmental Science and Technology 30, 2580-2585.

Ostro, B., Chestnut, L. (1998) Assessing the health benefits of reducing particulate matter air pollution in the United States. Environmental Research 76, 94-106.

Paatero, P. (1997) Least squares formulation of robust non-negative factor analysis. Chemometrics and Intelligent Laboratory Systems 37, 23-35.

Paatero, P., Tapper, U. (1994) Positive matrix factorization: a non-negative factor model with optimal utilization of error estimates of data values. Environmetrics 5, 111-126.

Pankow, J.F. (1994a) An absorption model of the gas/aerosol partitioning involved in the formation of secondary organic aerosol. Atmospheric Environment 28, 189-193.

Pankow, J.F. (1994b) An absorption model of the gas/aerosol partitioning of organic compounds in the atmosphere. Atmospheric Environment 28, 185-188.

Park, J.H., Goldstein, A.H., Timkovsky, J., Fares, S., Weber, R., Karlik, J., Holzinger, R. (2013) Eddy covariance emission and deposition flux measurements using proton transfer reaction - time of flight - mass spectrometry (PTR-TOF-MS): comparison with PTR-MS measured vertical gradients and fluxes. Atmospheric Chemistry and Physics 13, 1439-1456.

Perri, M.J., Seitzinger, S., Turpin, B.J. (2009) Secondary organic aerosol production from aqueous photooxidation of glycolaldehyde: Laboratory experiments. Atmospheric Environment 43, 1487-1497.

Prenni, A.J., DeMott, P.J., Kreidenweis, S.M., Sherman, D.E., Russell, L.M., Ming, Y. (2001) The effects of low molecular weight dicarboxylic acids on cloud formation. Journal of Physical Chemistry A 105, 11240-11248.

Prenni, A.J., DeMott, P.J., Kreidenweis, S.M. (2003) Water uptake of internally mixed particles containing ammonium sulfate and dicarboxylic acids. Atmospheric Environment 37, 4243-4251.

Raymond, T.M., Pandis, S.N. (2002) Cloud activation of single-component organic aerosol particles. Journal of Geophysical Research 107, doi:10.1029/2002JD002159

Robinson, A.L., Donahue, N.M., Shrivastava, M.K., Weitkamp, E.A., Sage, A.M., Grieshop, A.P., Lane, T.E., Pierce, J.R., Pandis, S.N. (2007) Rethinking organic aerosols: Semivolatile emissions and photochemical aging. Science 315, 1259-1262.

Tsigaridis, K., Kanakidou, M. (2003) Global modelling of secondary organic aerosol in the troposphere: a sensitivity analysis. Atmospheric Chemistry and Physics 3, 1849-1869.

Turpin, B.J., Saxena, P., Andrews, E. (2000) Measuring and simulating particulate organics in the atmosphere: problems and prospects. Atmospheric Environment 34, 2983-3013.

Ulbrich, I.M., Canagaratna, M.R., Zhang, Q., Worsnop, D.R., Jimenez, J.L. (2009) Interpretation of organic components from positive matrix factorization of aerosol mass spectrometric data. Atmospheric Chemistry and Physics 9, 2891-2918.

Yu, X.-Y., Lee, T., Ayres, B.R., Kreidenweis, S.M., Collett, J.L., Jr. (2006) Loss of fine particle ammonium from denuded nylon filters. Atmospheric Environment 40, 4797-4807.

Yuan, B., Hu, W.W., Shao, M., Wang, M., Chen, W.T., Lu, S.H., Zeng, L.M., Hu, M. (2013) VOC emissions, evolutions and contributions to SOA formation at a receptor site in eastern China. Atmospheric Chemistry and Physics 13, 8815-8832.

Zhang, J.Y., Hartz, K.E.H., Pandis, S.N., Donahue, N.M. (2006) Secondary organic aerosol formation from limonene ozonolysis: Homogeneous and heterogeneous influences as a function of NO_x. Journal of Physical Chemistry A 110, 11053-11063.

Zhang, Q., Jimenez, J., Canagaratna, M., Ulbrich, I., Ng, N., Worsnop, D., Sun, Y. (2011) Understanding atmospheric organic aerosols via factor analysis of aerosol mass spectrometry: a review. Analytical Bioanalytical Chemistry 401, 3045-3067.

(Received 4 July 2017, revised 12 September 2017, accepted 12 September 2017)